Published in final edited form as:
J Immunol. 2012 August 1; 189(3): 1133–1143. doi:10.4049/jimmunol.1003406.

Cathepsin B controls the persistence of memory CD8+ T lymphocytes[1]

Susan M. Byrne[*,†], **Anne Aucher**[‡], **Syarifah Alyahya**[*], **Matthew Elder**[*], **Steven T. Olson**[§], **Daniel M. Davis**[‡], and **Philip G. Ashton-Rickardt**[*,2]

[*]Section of Immunobiology, Division of Immunology and Inflammation, Department of Medicine, Faculty of Medicine, Imperial College London, London W12 0NN, UK.

[†]Committee on Immunology, University of Chicago, Chicago, IL 60637, USA.

[‡]Section of Immunology and Infection, Division of Cell and Molecular Biology, Imperial College London, London SW7 2AZ.

[§]Center for Molecular Biology of Oral Diseases, University of Illinois at Chicago, Chicago, IL 60612, USA.

Abstract

The persistence of memory T lymphocytes confers lifelong protection from pathogens. Memory T cells survive and undergo homeostatic proliferation (HSP) in the absence of antigen, although the cell intrinsic mechanisms by which cytokines drive the HSP of memory T cells are not well understood. We now report that lysosome stability limits the long-term maintenance of memory $CD8^+$ T cell populations. Serine protease inhibitor 2A (Spi2A), an anti-apoptotic cytosolic cathepsin inhibitor, is induced by both IL-15 and IL-7. Mice deficient in Spi2A developed fewer memory-phenotype $CD44^{hi}$ $CD8^+$ T cells with age, which underwent reduced HSP in the bone marrow. Spi2A was also required for the maintenance of central memory $CD8^+$ T cell populations after acute infection with Lymphocytic Choriomeningitis virus (LCMV). Spi2A-deficient antigen-specific $CD8^+$ T cell populations declined more than wild type competitors after viral infection, and were eroded further after successive infections. Spi2A protected memory cells from lysosomal breakdown by inhibiting cathepsin B. The impaired maintenance of Spi2A-deficient memory $CD8^+$ T cells was rescued by concomitant cathepsin B deficiency, demonstrating that cathepsin B was a physiological target of Spi2A in memory $CD8^+$ T cell survival. Our findings support a model in which protection from lysosomal rupture through cytokine-induced expression of Spi2A determines the long-term persistence of memory $CD8^+$ T cells.

Keywords

memory T cells; serine protease inhibitor; cathepsin B

Introduction

In order to provide lifelong immunity from subsequent re-infections, antigen-specific memory T lymphocytes develop an increased precursor frequency, a lower reactivation

[1]This work was supported by the National Institutes of Health grant AI45108, The Wellcome Trust, and Cancer Research UK (to P.G.A-R.) S.B. was supported by The Molecular and Cell Biology training grant at the Univ. of Chicago.

[2] Address correspondence to: P.G. Ashton-Rickardt, Section of Immunobiology, Division of Immunology and Inflammation, Department of Medicine, Faculty of Medicine, Imperial College London, London W12 0NN, UK. Phone: (+44) 20-8383-4135; Fax: (+44) 20-8383-2788; p.ashton-rickardt@imperial.ac.uk.

threshold, and a faster re-expansion capability compared to naive T cells (1). Once the memory $CD8^+$ T cell population has been established, its long-term maintenance depends on successful survival and homeostatic proliferation (HSP), a low level of regenerative cell division that is driven by cytokines rather than antigen. As different pathogens are encountered, memory $CD8^+$ T cell populations from earlier infections (which have not re-encountered antigen) will decline in frequency (2).

Antigen stimulates $CD8^+$ T cells to proliferate and differentiate into short-lived effector cytotoxic T lymphocyte (CTL) and the precursors of long-lived memory cells (3, 4). After this expansion phase, short-lived CTL (IL-$7R^{lo}$ Killer cell lectin-like receptor $G1^{hi}$ ($KLRG1^{hi}$) undergo programmed cell death (PCD), whereas memory precursor effector cells (IL-$7R^{hi}$ ($KLRG1^{lo}$) escape PCD and go on to persist as memory cells (5). Memory $CD8^+$ T cells represent a heterogeneous population, and the persistence of different subsets can vary. Central memory T cells (T_{CM}) are long-lived, express CD62L, predominate in lymphoid organs, and have the capacity for recall proliferation upon subsequent re-encounter with antigen (6, 7). T_{CM} cells exhibit high rates of HSP and so are thought to be capable of long-term persistence (6, 7). Eventually – around one year post infection in the mouse – the long-term antigen-specific memory $CD8^+$ T cell population will become almost entirely $CD62L^{hi}$ (4).

The overall level of memory $CD8^+$ T cells is largely dictated by the cytokines IL-7 and IL-15, which drive HSP preferentially in the bone marrow (8-11). These survival cytokines induce the expression of the anti-apoptotic molecules Bcl-2, Bcl-X_L, and Mcl-1 in memory $CD8^+$ T cells (12-14). However, the nature of the cell intrinsic mechanisms that control the survival and HSP of long-term memory T lymphocytes is poorly understood (15).

Lysosomal cathepsins are responsible for the proteolytic degradation that underpins many cellular processes. The targets and functions of cathepsins are determined by sub-cellular localization. In lysosomal vesicles, cathepsins are required for protein turnover, antigen processing in the endoplasmic reticulum, and the degradation of the contents of autophagosomal vesicles (16, 17). In response to a variety of stimuli, such as TNF-α (18-20) and Reactive Oxygen Species (ROS) (21-23), cathepsins are released from permeabilized lysosomes into the cytosol.

Once in the cytosol, cathepsins can trigger several death pathways, both dependent and independent of mitochondria. Cathepsins can cleave and activate Bid (24, 25) and indirectly activate Bax (26, 27). Cysteine cathepsins can also degrade Bcl-2, Bcl-X_L, and Mcl-1 (28). This can cause further mitochondrial membrane permeabilization, which releases ROS that can feed back to the lysosomes and induce further lysosomal permeabilization. Cysteine cathepsins can also activate the caspase pathway by degrading the caspase inhibitor XIAP (28). Chemical cathepsin inhibitors can protect cells from death receptor- or mitochondrial-induced apoptosis; however, the predominance of these different apoptotic pathways depends on the stimulus and cell type. The physiological downstream targets for cathepsins *in vivo* are not well understood.

We have identified Serine Protease Inhibitor 2A (Spi2A) as a physiological inhibitor of the lysosomal pathway of death in mice (29). Spi2A, encoded by the *Serpina3g* gene on mouse chromosome 12 (30), is unusual for a serine protease inhibitor (serpin) in that that it inhibits cysteine cathepsins and resides in the cytosol and nucleus (31). Spi2A was first identified in $CD8^+$ T cells due to its particular gene expression pattern: it has a low level of expression in naive cells; is up-regulated in effector cells, especially in IL-$7R^{hi}$ memory cell precursors; and continues to be expressed in memory $CD8^+$ T cells, months after the infection has subsided (29). Over-expressing *Spi2A* enhances the initial development of memory $CD8^+$ T

cells (29), but whether Spi2A plays a non-redundant role in maintaining long-term memory $CD8^+$ T cells is unclear.

To examine the role of Spi2A in memory $CD8^+$ T cell survival, we examined Spi2A knockout (Spi2A KO) mice (32). We observed an age-dependent deficit and impaired HSP of both memory-phenotype and LCMV-specific memory $CD8^+$ T cells in Spi2A KO mice. Competitive adoptive transfer experiments demonstrated that Spi2A exerted a cell autonomous survival effect on memory $CD8^+$ T cells and protected from erosion in cell number after re-infection. *Spi2A* transcription was induced by cytokines critical for regulating memory $CD8^+$ T cells, including IL-15. Confocal microscopy of memory cells revealed that Spi2A protected lysosomes from cathepsin B driven permeabilization. Complementing Spi2A KO mice with cathepsin B deficiency restored lysosome integrity along with the maintenance and HSP of memory CD8 T cells *in vivo*, showing that increased cathepsin B activity was responsible for these effects. Our findings provide evidence that protection from lysosomal PCD regulates the homeostatic persistence of memory $CD8^+$ T cells.

Materials and Methods

Mouse Strains

Spi2A KO mice were (32) crossed with P14 transgenic mice (33) and *cathepsin B*$^{-/-}$ mice (34), all on the C57BL/6 background. CD45.1 congenic C57BL/6 mice (Jackson Labs) were also crossed as described. C57BL/6, DBA/2, and Thy1.1$^+$ congenic C57BL/6 mice were purchased from Jackson Labs via Charles River UK. Female mice were used at 16-weeks-old unless indicated otherwise. All mice were maintained in accordance with Univ. of Chicago IACUC and UK Home Office regulations.

Tissue Preparation

Peripheral blood was drawn by tail vein puncture. Spleen, inguinal lymph nodes, and bone marrow from the femur were harvested using standard techniques. Red blood cells were lysed using Tris-buffered ammonium chloride. Intrahepatic lymphocytes and lung lymphocytes were isolated by first perfusing the organs with PBS. These organs were ground through a 70 μm cell strainer (BD), washed thrice with PBS, and purified using Lympholyte-M (CedarLane). Cell counts were determined by flow cytometry using Caltag counting beads (Invitrogen).

Flow Cytometry

Monoclonal antibodies against mouse CD8, CD4, CD44, CD45.1, CD45.2, IL-7R, and KLRG1 were used. All antibodies were purchased from BD or eBioscience. Stains were performed in PBS supplemented with 0.2% BSA (Sigma), 10% normal goat serum (Invitrogen), and anti-CD16/32 F_c block (eBioscience). Antigen-specific T cells were stained using tetramers against the LCMV gp33 epitope on H-2D^b (Beckman Coulter). BrdU incorporation was measured using the FITC BrdU Flow Kit (BD). Flow cytometry was done on a FACS Cyan (Beckman Coulter) and cell sorting was done on a FACS Aria (BD).

Real time PCR

mRNA was isolated using the Qiagen micro RNA kit. cDNA was prepared using the Invitrogen Superscript III kit and oligo(dT). Real-time PCR reactions were run using the SYBR Green PCR Master mix (Applied Biosystems) on a 7900HT Fast Real-Time PCR System (Applied Biosystems). Primer sequences for *Serpina3g, Serpina3f, vimentin*, and *β2microglobulin* come from (35).

Cytokine up-regulation

$CD44^{hi}$ $CD8^+$ cells were purified by anti-CD8α magnetic microbeads (Miltenyi) and FACS purified from three pooled wild type mice (>98% purity). 10^4 cells were cultured in 100 μl complete DMEM-10 without cytokine for 4 hours, and then cultured in 100 ng / ml of IL-2, IL-7, or IL-15 (eBioscience) for the indicated periods.

Memory T cell assays

To measure T cell proliferation, mice were fed 0.8 mg/ml BrdU in drinking water for 7 days. For competition experiments, $CD8^+$ T cells were purified using anti-CD8α magnetic microbeads (Miltenyi) from wild type $P14^+$ ($CD45.1^+$) and Spi2A KO $P14^+$ ($CD45.2^+$) mice (>90% purity). The cells were combined in equal amounts and 5000 $P14^+$ $CD8^+$ cells were co-adoptively transferred into wild type recipients ($CD45.1^+2^+$). Mice were infected *i.p.* with 2×10^5 PFU LCMV Armstrong. $P14^+$ cells were identified by flow cytometry using antibody and gp33/H-$2D^b$-tetramer staining (5, 36). Secondary and tertiary adoptive transfers were performed > 200 days p.i. using the same procedure with donor $CD8^+$ splenocytes taken from the previous recipients.

Live-Cell Imaging

Cells were imaged in eight-well chambered coverglasses (Chambered Borosilicate Coverglass; Lab-Tek) pre-coated with 10 μg / ml fibronectin (Sigma). Cells were imaged at 37°C, 5% (v/v) CO_2 by resonance laser scanning confocal microscopy (TCS SP5 RS; Leica) using an excitation wavelength of 488 nm with a 63× water immersion objective (N.A. = 1.2) and analyzed (Volocity and Image J; National Institutes of Health). Acidic lysosomes were visualized by staining with LysoTracker Green DND-26 according to supplier's instructions (Molecular Probes).

Recombinant Spi2A expression and purification

Spi2A was expressed in *E. coli* as a GST fusion protein with a factor Xa cleavage site. The protein was purified from cell extracts by batch adsorption to Glutathione-Sepharose beads in 20 mM sodium phosphate buffer, 0.1 M NaCl, 0.1 mM EDTA containing 15 mM PMSF, 5 mM DTT and 1% Triton X-100. Adsorbed beads were packed into a column and washed with 10 volumes of buffer containing 1 M NaCl followed by 10 volumes of original buffer with 0.1 M NaCl. The fusion protein was then eluted in buffer containing 15 mM reduced glutathione and detected by SDS-PAGE. The GST tag was cleaved by incubation of ~300 μg/ml protein with ~10 μg/ml factor Xa for 4 hours in sodium phosphate buffer without PMSF, DTT, or Triton followed either by inactivation of the factor Xa with 100 μM Glu-Gly-Arg-chloromethylketone or adsorption of the enzyme with soybean trypsin inhibitor-agarose beads. After dialysis into 20 mM Tris buffer, pH 7.4, containing 1 mM EDTA and 1 mM DTT, the protein was loaded onto a mono Q column and the Spi2A eluted with a linear NaCl gradient from 0-0.2 M in buffer. Spi2A fractions were detected by SDS-PAGE and cathepsin L inhibitory activity, pooled, concentrated, and dialyzed into storage buffer consisting of 0.1 M HEPES, 0.1 M NaCl, 5 mM DTT, pH 7.4. Concentrations of Spi2A were determined from the 280 nM absorbance based on an extinction coefficient of 26,300 $M^{-1}cm^{-1}$ calculated from the amino acid sequence (37).

Cathepsin Activity Assays

The buffers utilized for characterizing the kinetics and stoichiometry of Spi2A inhibition of cathepsins were based on those found to yield optimal enzyme stability: Cathepsins L, B, and papain: 20 mM sodium phosphate, 0.1 M NaCl, 0.1 mM EDTA, 0.1% PEG 8000, 5 mM DTT, pH 6; Cathepsin S: 20 mM sodium phosphate, 0.1 M NaCl, 0.1 mM EDTA, 0.1% PEG 8000, 5 mM DTT pH 7.4; Cathepsins H, V, and K: 0.1 M sodium acetate, 1 mM

EDTA, 0.1% PEG 8000, 5 mM DTT, pH 5.5. It should be noted that the kinetics of cathepsin L inhibition by Spi2A were found to be independent of pH in the 5.5-7.4 range. All cathepsins were activated by diluting stock solutions into buffer containing 5 mM DTT and incubating for 5-15 min on ice.

The molar concentrations of active cathepsins were determined by active-site titration with E64 (38). Briefly, ~50-100 nM solutions of enzyme were incubated with increasing molar ratios of E64 for a time shown to yield complete inhibition based on measured second order rate constants for E64 inhibition. Residual cathepsin activity was then measured in standard fluorogenic substrate assays (described below) and plotted as a function of E64 concentration. The x-intercept corresponding to complete inhibition yielded the active enzyme concentration. Turnover numbers for hydrolysis of substrates by cathepsins under standard conditions (described below) were calculated based on active-site titration data and served as calibrators of functional enzyme activity in all experiments.

To measure the kinetics of inhibition, reactions were done at 25°C under pseudo-first order conditions in which the concentration of Spi2A was at least 5-10 times greater than the concentration required to completely inhibit the enzyme activity (39). Reactions were initiated by adding a small aliquot of cathepsin to a solution of Spi2A in 100 μl of reaction buffer and then quenched after varying reaction times by adding 900 μl of 50 μM fluorogenic substrate in reaction buffer. The residual enzyme activity was measured from the initial linear rate of fluorescence increase (380 nm excitation, 440 nm emission) due to hydrolysis of the substrate. The time-dependent loss in enzyme activity was fit by a single exponential decay function to obtain the pseudo-first order inhibition rate constant. This was divided by the Spi2A concentration to give the second order inhibition rate constant. Observed pseudo-first order rate constants were found to increase in proportion to the Spi2A concentration in all cases, confirming that all reactions were bimolecular.

To measure the stoichiometry of inhibition, 100 nM cathepsin was incubated with increasing molar ratios of Spi2A to cathepsin (0-500 nM) in 50 μl reaction volumes at 25°C for a time that yielded complete reaction (>90%) based on measured second order rate constants and over which enzyme activity remained stable. Residual enzyme activity was then measured by adding 950 μl of 50 μM substrate directly to the reaction mixture or to a suitable dilution of this mixture and the initial rate of substrate hydrolysis was measured as in the kinetics experiments. A plot of residual enzyme activity versus molar ratio of Spi2A to enzyme concentration yielded the stoichiometry of inhibition from the x-axis intercept.

Results

Reduced levels of endogenous memory-phenotype CD44^{hi} CD8^{+} T cells in Spi2A KO mice

We have reported the complete absence of *Spi2A* mRNA expression in Spi2A KO mice (32), whereas the expression of the linked *Serpina3f* gene (30) was not affected. Spi2A KO mice are viable and exhibit no gross differences in the levels of erythroid, myeloid, or lymphoid cells and possess normal proportions of CD8^{+}, CD4^{+}, and B220^{+} lymphocytes (Supplemental Tables 1 and 2). However, Spi2A KO mice develop fewer memory-phenotype CD44^{hi} CD8^{+} T cells with age. The activation marker CD44 is up-regulated by memory-phenotype T cells after the recognition of endogenous antigens (40). Among T cells, the proportion of CD44^{hi} memory-phenotype cells increases with age and antigen experience, as the proportion of CD44^{lo} naive cells declines (41). 12-week-old Spi2A KO mice possessed similar proportions of CD44^{hi} peripheral blood leukocytes (PBL); however, at 16 weeks, Spi2A KO mice developed a significantly lower CD44^{hi} proportion of CD8^{+} PBL compared to wild type mice (Figure 1A and 1B). Spi2A KO mice also showed a significant reduction in the number of memory-phenotype CD44^{hi} CD8^{+} T cells in the bone

marrow at 15-weeks-old ($P = 0.0008$) (Figure 1C). Lower $CD44^{hi}$ proportions were also found in the spleen, lymph nodes, and intrahepatic lymphocytes (IHL), although these differences were not consistently statistically significant (data not shown). No differences were observed in younger mice (9 weeks), demonstrating an age-dependent phenotype (Figure 1C). Furthermore, the defect in memory-phenotype T cell levels in Spi2A KO mice was specific to $CD8^+$ T cells, as the level of $CD44^{hi}$ $CD4^+$ cells was not affected (Figure 1B and 1C). Thus, Spi2A-deficiency results in an age-specific decrease in the level of memory-phenotype $CD44^{hi}$ $CD8^+$ T cells.

Impaired homeostatic proliferation of Spi2A KO memory-phenotype $CD44^{hi}$ $CD8^+$ T cells

Memory $CD8^+$ T cells undergo a low rate of cell division in the absence of overt antigen stimulation, referred to as homeostatic proliferation. The bone marrow is the preferred site for the homing and HSP of memory $CD8^+$ T cells (8-10). The $CD44^{hi}$ $CD8^+$ T cells in the bone marrow of 15-week-old Spi2A KO mice had significantly ($P = 0.0008$) lower levels of HSP measured by BrdU incorporation *in vivo* (40) (Figure 1C). This requirement for Spi2A was also specific for $CD8^+$ T cells, as $CD44^{hi}$ $CD4^+$ T cells in the same mice showed no HSP difference (Figure 1C). Naive $CD44^{lo}$ cells (either $CD8^+$ or $CD4^+$) showed very little BrdU incorporation, consistent with previous reports (42). We conclude that Spi2A is required for the homeostatic proliferation of memory-phenotype $CD44^{hi}$ $CD8^+$ T cells.

Memory $CD8^+$ T cells require the cytokines IL-7 and IL-15 for survival and HSP in the bone marrow; however, they do not require continued TCR stimulation (43). Spi2A expression is up-regulated upon NF-κB activation, yet Spi2A expression continues long after infection in memory $CD8^+$ T cells (29, 31). We found that IL-7 and IL-15, as well as IL-2, induced the expression of *Serpina3g* mRNA in $CD44^{hi}$ $CD8^+$ T cells *in vitro* in the absence of additional TCR stimulation (Figure 1D). We conclude that Spi2A is up-regulated by these cytokines to ensure the maintenance of memory $CD8^+$ T cells.

Spi2A is required for the long-term maintenance and HSP of LCMV-specific memory $CD8^+$ T cells, but is redundant for determining the level of memory cell precursors

While memory-phenotype $CD44^{hi}$ $CD8^+$ T cells, which are generally stimulated by environmental antigens, share many similarities with antigen-specific memory $CD8^+$ T cells stimulated by experimental infections, they possess some differences in their maintenance requirements (43). To address the role of Spi2A in an antigen-specific memory $CD8^+$ T cell response, we examined $CD8^+$ T cells after acute infection with Lymphocytic Choriomeningitis virus (LCMV) (29, 36). Tetramer staining was used to identify $CD8^+$ T cells specific for the gp33 LCMV epitope after LCMV infection (Figure 2A). We further examined these antigen-specific $CD8^+$ T cells by examining their surface expression of phenotypic markers. These markers define $CD8^+$ subsets that possess various functional properties: a memory precursor phenotype ($IL\text{-}7R^{hi}$ $KLRG1^{lo}$) or a central memory (T_{CM}) ($CD62L^+$) phenotype. With time, the long-term antigen-specific memory $CD8^+$ T cell population will gradually become $CD62L^{hi}$, $IL\text{-}7R^{hi}$, and $KLRG1^{lo}$ (4, 5, 44).

Both wild type and Spi2A KO mice showed a similar expansion of antigen-specific $CD8^+$ T cells 8 days post infection (p.i.) (Figure 2B). They also showed a similar subsequent contraction in the number of LCMV-specific $CD8^+$ T cells (Figure 2B). In addition, we did not observe any difference in the proportion of $IL\text{-}7R^{hi}$ $KLRG1^{lo}$ memory precursor cells among the gp33-specific $CD8^+$ population at any time between wild type and Spi2A KO mice (Figure 2B). Therefore, we found no evidence to indicate that Spi2A is solely required for the survival of early memory precursor cells. This contradicts an earlier report of decreased CTL levels after antisense knock down of *Spi2A* mRNA (29). We have since discovered that other *Serpina3* family genes are also up-regulated in activated T cells

(Supplemental Figure 1). These genes are nearly identical to Spi2A (>90% homology in the case of *Serpina3f*) except for some variability in the region encoding the reactive center loop, which determines the specificity of protease inhibition (30). Therefore, the earlier antisense approach likely also reduced the expression of homologous, but distinct, mRNAs related to *Spi2A*. In Spi2A KO mice, Spi2A mRNA expression was specifically ablated by targeting *Serpina3g* exon 4 (32). Our present study reveals redundancy between Spi2A and other serpins in determining the survival of memory precursor cells in the clonal burst phase of the $CD8^+$ immune response.

However, from d130 p.i. onwards, we observed significantly lower numbers of gp33-specific memory $CD8^+$ T cells in Spi2A KO compared with wild type mice (spleen: $P = 0.05$; ILN: $P = 0.04$) (Figure 2B). Throughout the antigen-specific $CD8^+$ T cell response, the proportion of IL-$7R^{hi}$ $KLRG1^{lo}$ cells remained similar between wild type and Spi2A KO mice, and by d130, these cells were mainly IL-$7R^{hi}$ $KLRG1^{lo}$ (Figure 2B). Therefore, the absolute number of IL-$7R^{hi}$ $KLRG1^{lo}$ memory $gp33^+$ $CD8^+$ cells also decreased correspondingly in Spi2A KO mice (spleen: $P = 0.02$; ILN: $P = 0.03$).

Yet, in the long-term memory phase after infection, the proportion of central memory $CD62L^{hi}$ cells in the $gp33^+$ $CD8^+$ T cell population was significantly reduced in Spi2A KO mice compared to wild type controls (spleen: $P = 0.02$; bone marrow $P = 0.02$) (Figure 2C). The absolute number of T_{CM} $gp33^+$ $CD8^+$ T cells was also significantly decreased in Spi2A KO mice compared to wild type (spleen: $P = 0.04$; bone marrow: $P = 0.04$) (Supplemental Table 3).

Furthermore, we observed a significant decrease in the percentage of $BrdU^+$ memory $gp33^+$ $CD8^+$ T cells in the bone marrow of Spi2A KO mice ($P = 0.04$) (Figure 2D). This proliferation difference occurred even within the $CD62L^+$ $gp33^+$ $CD8^+$ cell subset, demonstrating that this effect was not simply due to Spi2A KO mice having fewer T_{CM} (Figure 2D). Therefore, Spi2A is solely required for the full long-term maintenance and HSP of antigen-specific memory $CD8^+$ T cells *in vivo*.

Cell intrinsic effect of Spi2A on memory $CD8^+$ T cells

To isolate the cell-intrinsic requirements for Spi2A in memory $CD8^+$ T cell development, Spi2A-deficient $gp33^+$ $CD8^+$ T cells were examined alongside competing wild type $gp33^+$ $CD8^+$ T cells in a shared wild type environment. Naïve Spi2A KO ($CD45.2^+$) $CD8^+$ T cells expressing the P14 transgenic TCR specific for the LCMV peptide gp33/H-$2D^b$ (5) were mixed with wild type $CD45.1^+$ $P14^+$ $CD8^+$ T cells in a 1:1 ratio. 5000 $P14^+$ $CD8^+$ cells were adoptively transferred into $CD45.1^+2^+$ hybrid congenic C57BL/6 recipients, which were infected with LCMV (Figure 3A). Spi2A-deficient and wild type donor $P14^+$ $CD8^+$ T cells were identified by the expression of congenic markers (Figure 3B). The kinetics of LCMV-specific $CD8^+$ T cell numbers during the expansion (d 8 p.i.), contraction (d 15 p.i.), and memory phases (d 70 p.i. onwards) matched those previously reported for this virus model (29, 36) (Figure 3C). The ratio of Spi2A KO to wild type $P14^+$ cells remained equivalent during the expansion phase; however, during the memory phase, the ratio of Spi2A KO to wild type $P14^+$ cells dropped to less than 1 in all of the lymphoid organs studied (Figure 3C). Therefore, our findings indicate that, although Spi2A was not solely required for CTL during the initial clonal expansion (5, 36), Spi2A was required for ensuring the continued maintenance of LCMV-specific memory $CD8^+$ T cells. These findings match our earlier results in intact LCMV-infected Spi2A KO mice (Figure 2B).

The ratio of $P14^+$ cells in the bone marrow during the expansion and contraction phases differed from the other organs studied. It has since been reported that polymorphisms present in the CD45.1 congenic interval impair $CD45.1^+$ hematopoietic stem cell homing to

the bone marrow, independent of apoptosis or proliferation (45). Similarly, these polymorphisms also appear to impair CD45.1$^+$ CD8$^+$ T cell migration to the bone marrow during the contraction phase. However, even with such an impairment, CD45.1$^+$ wild type P14$^+$ CD8$^+$ T cells still out-competed their Spi2A KO CD45.2$^+$ counterparts, as the Spi2A KO to wild type ratio of P14$^+$ cells eventually declined to below 1 in the bone marrow during the memory phase (Figure 3C).

As in complete Spi2A KO mice, the adoptively transferred Spi2A-deficient memory P14$^+$ CD8$^+$ T cells underwent less homeostatic proliferation compared to their wild type counterparts in the same mice (Figure 3D). We conclude that Spi2A is required in a cell intrinsic manner to ensure the maintenance and HSP of memory CD8$^+$ T cells following an acute LCMV infection.

Spi2A deficiency leads to erosion of antigen-specific memory CD8$^+$ T cell populations after successive infections

An important physiological requirement for memory T cell populations is persistence through multiple rounds of re-infection (2). Since Spi2A acted to ensure the maintenance and HSP of primary memory CD8$^+$ T cells, we wanted to determine if it was also required to ensure the survival of secondary and tertiary CD8$^+$ memory cells. Memory P14$^+$ CD8$^+$ splenocytes from an initial adoptive transfer (1°, as described above in Figure 3) were isolated and re-transplanted into naive CD45.1$^+$2$^+$ recipients (Figures 4A and 4B). Upon this secondary adoptive transfer (2°) and re-infection, the ratio of Spi2A KO: wild type P14$^+$ CD8$^+$ cells further decreased to 0.51 after 231 days (Figure 4C). After a third successive adoptive transfer (3°) into naive CD45.1$^+$2$^+$ recipients, the ratio of Spi2A KO: wild type P14$^+$ CD8$^+$ cells decreased again to 0.25 after 93 d (Figure 4C). Control experiments transferring 5000 memory gp33$^+$ CD8$^+$ cells from either wild type or Spi2A KO mice into congenic recipients revealed equal amounts of re-expansion after LCMV infection (Supplemental Figure 2). As we had observed with primary memory cells (Figure 3), Spi2A is required to maintain secondary and tertiary memory CD8$^+$ T cells. Therefore, Spi2A protects the antigen-specific memory CD8$^+$ T cell population from erosion after successive rounds of viral infection.

Cathepsin B-driven lysosomal permeabilization in Spi2A KO memory cells

Lysosomal membrane permeabilization (LMP) results in the release of cathepsins into the cytosol and the induction of cell death (46). The release of cathepsin B also degrades and permeabilizes the lysosomal membrane in a positive feedback loop (31, 47). Lysosomes in live FACS-purified CD8$^+$ splenocytes were marked with Lysotracker Green, a fluorescent probe which accumulates in intact acidic organelles, and then visualized by confocal fluorescence microscopy (Figure 5A). Lysotracker labelling is lost upon LMP and the resulting increase in pH (48). Wild type memory-phenotype CD44^{hi} CD8$^+$ cells possessed significantly greater Lysotracker fluorescence compared to naive CD44^{lo} CD8$^+$ cells (P = 0.0001) (Figure 5B), due to an increased number of acidic intact lysosomes indicated by a higher number of Lysotracker puncta (Figure 5A). This indicates an increased number of secretory lysosomes and/or level of metabolic activity in memory-phenotype versus naïve CD8$^+$ T cells (49).

Significantly fewer intact lysosomes were found in memory-phenotype CD8$^+$ cells from Spi2A KO mice (P = 0.0001) (Figure 5B), with clearly fewer puncta of Lysotracker visible (Figure 5A). To determine whether increased cathepsin B activity contributed to LMP in Spi2A KO memory-phenotype CD8$^+$ cells, we crossed Spi2A KO mice to Cathepsin B knockout mice (Cath B KO) (34). In the absence of cathepsin B, the number of lysosomes in Spi2A KO × Cath B KO memory-phenotype CD8$^+$ cells returned to the wild type level

(Figure 5A and 5B). Thus, the reduced number of lysosomes in Spi2A KO mice was not due to impaired development or organelle organization. Rather, Spi2A ensures lysosomal integrity by preventing cathepsin B-mediated LMP and the resulting initiation of the lysosomal pathway of death.

Spi2A is a direct inhibitor of cathepsin B

To confirm that Spi2A is a direct inhibitor of cathepsin B, we showed that recombinant Spi2A produced from *E. coli* inhibited cathepsin B with a stoichiometry of 10:1 giving a corrected rate of 6×10^3 M^{-1} s^{-1} (Figure 6A and 6B)(50). Examination of a panel of papain-like cysteine cathepsins gave a range of rates and stoichiometries of inhibition by Spi2A (Figure 6C). SDS-PAGE revealed the presence of intact cathepsin B and cleaved Spi2A as the only visible products of the reaction because of the instability of serpin-cysteine protease complexes to SDS denaturation (Figure 6D) (51). Therefore, as has been observed with other cross class-specific serpins, Spi2A inhibits cathepsin B by forming a serpin: protease inhibitory complex whose thioester linkage is unstable under reducing conditions (52).

Cathepsin B-deficiency restores the endogenous memory-phenotype $CD44^{hi}$ $CD8^+$ T cell population in Spi2A KO mice

We determined whether cathepsin B was a physiological target for the Spi2A-mediated maintenance of memory $CD8^+$ T cells *in vivo*. To examine this, we crossed Spi2A KO mice to Cathepsin B-deficient mice (Cath B KO) (34). Cath B KO mice appear normal, but are resistant to TNF-α-induced hepatocyte apoptosis (20). Flow cytometry staining revealed a similar number of memory-phenotype $CD44^{hi}$ $CD8^+$ T cells in the bone marrow of 15-week-old Spi2A KO × Cath B KO mice compared to wild type controls. Cath B KO mice also possessed wild type levels of memory-phenotype $CD44^{hi}$ $CD8^+$ T cells. Therefore, cathepsin B deficiency alone did not produce a global increase in cell number (Figure 7A). Rather, cathepsin B deficiency specifically rescued the memory-phenotype $CD44^{hi}$ $CD8^+$ population in Spi2A KO × Cath B KO mice. In addition to rescuing the number of cells, cathepsin B deficiency also restored the impaired homeostatic proliferation of memory-phenotype $CD44^{hi}$ $CD8^+$ cells in Spi2A KO mice (Figure 7B). Therefore, the inhibition of cathepsin B is a physiological mechanism by which Spi2A ensures the maintenance and HSP of endogenous memory-phenotype $CD8^+$ T cells.

Cathepsin B-deficiency rescues the LCMV-specific central memory $CD8^+$ T cell population in Spi2A KO mice

Next, we determined whether cathepsin B inhibition was a mechanism by which Spi2A maintained the level and self-renewal of LCMV-specific memory $CD8^+$ T cells. Spi2A KO × Cath B KO mice and Cath B KO mice were infected with LCMV and analyzed by flow cytometry after 130 d p.i. as in Figure 2. Spi2A KO × Cath B KO mice possessed wild type numbers of memory gp33 $tetramer^+$ $CD8^+$ T cells (Figure 8A). As we observed for endogenous memory-phenotype $CD44^{hi}$ $CD8^+$ T cells (Figure 7), cathepsin B deficiency itself did not increase the LCMV-specific memory $CD8^+$ T cell population above wild type levels (Figure 8A). Furthermore, the proportion of $CD62L^+$ T_{CM} within the antigen-specific memory $CD8^+$ T cell population in both Spi2A KO × Cath B KO and Cath B KO mice remained at wild type levels (Figure 8B). In addition to restoring the level of LCMV-specific memory $CD8^+$ cells, cathepsin B deficiency also corrected the defective homeostatic proliferation in the bone marrow (Figure 8C). We conclude that inhibition of cathepsin B by Spi2A ensures the maintenance and HSP of long-lived LCMV-specific memory $CD8^+$ T cells.

The inhibition of cathepsin B by Spi2A in memory $CD8^+$ T cells was also cell-intrinsic, as demonstrated by the equivalent survival of Spi2A KO × Cath B KO compared to wild type

memory $P14^+$ $CD8^+$ T cells in competitive adoptive transfer experiments >70 d after LCMV infection (Figure 7C). Likewise, the ratio of Cath B KO to wild type memory $P14^+$ $CD8^+$ T cells also remained unchanged (Figure 7C). The cell-intrinsic effect of Spi2A's inhibition of cathepsin B extended to homeostatic proliferation, which was also restored to a wild type level in Spi2A KO × Cath B KO $P14^+$ $CD8^+$ T cells in the bone marrow (Figure 7D). Therefore, we conclude that Spi2A can act directly within $CD8^+$ T cells to inhibit cathepsin B and ensure the survival and self-renewal of long-term memory cells.

Discussion

Memory T lymphocytes persist for the life of the organism to retain the history of previous pathogen encounters. Survival cytokines (including IL-7 and IL-15) control the homeostasis of long-term memory $CD8^+$ T cells and yet the cell intrinsic protective mechanisms that they trigger to regulate these populations are poorly understood. We present a model for the long-term maintenance of memory $CD8^+$ T cell populations whereby these cytokines induce Spi2A to counteract the limitation placed on persistence by lysosomal permeabilization.

Previous work from our laboratory has shown that reducing Spi2A expression using an antisense message decreases the number of CTL and memory $CD8^+$ T cells (29). This is in contrast with our current findings with Spi2A KO mice, which show that the level of CTL is not affected but that only memory $CD8^+$ T cells are affected. Other homologous *Serpina3* family genes, distinguished by their unique reactive centers (30), are also up-regulated by activated T cells (Supplemental Figure 1). Therefore, a major shortcoming of the earlier study was that the antisense approach most likely knocked down the expression of homologous, but distinct mRNAs related to Spi2A. The knockout strategy in the present study specifically ablated Spi2A mRNA expression by targeting *Serpina3g* exon 4, and so resolved the shortcomings of the earlier approach.

While Spi2A over expression can increase the number of CTL during clonal expansion (29), we now show that Spi2A is uniquely required for the maintenance, although not the development of, memory $CD8^+$ T cells. This requirement was most pronounced in T_{CM}, which exhibit long-term persistence and homeostatic proliferation to provide lasting immunity. Adoptive transfer competition experiments demonstrated that Spi2A not only controlled the survival of memory $CD8^+$ T cells after an initial infection, but also prevented the erosion of this population after additional challenges. This predicts that protection from cathepsin B may be important in preserving memory $CD8^+$ T cells after repeated infection with heterologous viruses (2).

We show that Spi2A is required to maintain intact lysosomes in memory-phenotype $CD8^+$ cells. The rescue of the levels of intact lysosomes in Spi2A KO × Cath B KO $CD44^{hi}$ $CD8^+$ cells demonstrated that cathepsin B release is a cause as well as a consequence of LMP in T cells. Although it is well established that lysosomal cathepsin B triggers PCD (46), the anti-apoptotic Bcl-2 family members that can be cleaved and inactivated by isolated cathepsin B *in vitro* (28) have yet to be shown to be targets *in vivo*. Spi2A acts in the cytosol to inhibit cysteine cathepsins after lysosomal permeabilization and protects fibroblasts from downstream PCD (31). Although Spi2A KO memory-phenotype $CD8^+$ T cells possess fewer intact lysosomes, we did not observe any difference in the protein levels of Bcl-2, Bcl-X_L, Mcl-1, or Bim (Supplemental Figure 3A). Therefore at this time, the downstream death pathways triggered by LMP in Spi2A KO memory $CD8^+$ T cells are not clear. The decrease in the number of intact lysosomes could also limit the ability of Spi2A KO memory $CD8^+$ T cells to stave off PCD through the degradation of the contents of autophagosomal vesicles (16, 17, 53).

The resulting cathepsin B amplification loop for LMP may explain why Spi2A deficiency results in impaired maintenance of memory $CD8^+$ T cells despite the relatively slow kinetics for recombinant Spi2A inhibition of purified cathepsin B. Spi2A inhibition of cathepsin B *in vivo* may also occur through faster kinetics and a lower stoichiometry of protease inhibition than that measured *in vitro* because of unknown cofactor molecules that localize or activate the reacting proteins – a common feature of other serpin-protease reactions (50). Since Spi2A has the capacity to inhibit several cathepsins (Figure 6), Spi2A may also be required to protect cells from other cathepsins. Spi2A over expression in $CD8^+$ T cells increases the proportion of surviving memory cells (29); however, cathepsin B-deficient memory $CD8^+$ T cells only showed wild type levels of survival (Figures 7 and 8). The total balance of cathepsin activity, and not cathepsin B exclusively, could be responsible for the Spi2A KO phenotype. However, since cathepsin B deficiency was sufficient to restore the number and HSP of Spi2A-deficient memory CD8 T cells, the inhibition of another cathepsin may not be physiologically relevant in this context.

Another anti-apoptotic serpin, Serine Protease Inhibitor 6 (Spi6), protects CTL from granzyme B by maintaining the integrity of lysosomal-like cytotoxic granules (54). Spi2A and Spi6 appear to be similar in the way they protect $CD8^+$ T cells from the breakdown of lysosomal vesicles. However, Spi6 ensures CTL survival and thereby determines the size of the clonal burst (54), but plays no role in continued memory $CD8^+$ T cell survival (36). Conversely, Spi2A ensures memory $CD8^+$ T cell maintenance and thereby determines the size of the memory pool, but has no effect on CTL and the clonal burst. This division of labor between Spi6 and Spi2A presumably reflects the relative importance of different executioner proteases (granzyme B for CTL; cathepsin B for memory $CD8^+$ cell) in controlling $CD8^+$ T cell survival after viral infection.

While the effector memory ($CD62L^-$) $CD8^+$ T cell population may expand after heterologous infections, the total number of central memory $CD8^+$ T cells remains fixed (55). The cytokines IL-7 and IL-15 are important for the survival and homeostasis of T_{CM} (55-58). However, the cell intrinsic mechanisms by which these cytokines ensure memory $CD8^+$ T cell survival have remained unclear. IL-7 and IL-15 signaling up-regulates expression of other anti-apoptotic molecules including Bcl-2 and Bcl-X_L (43). However, over expression of Bcl-2 or Bcl-X_L did not affect the level of memory $CD8^+$ T cells *in vivo* (59, 60). IL-7 also induces Mcl-1, which is also required for T cell survival (13), but a role in memory $CD8^+$ T cell homeostasis has not been tested. We show that IL-7 and IL-15 signaling also up-regulates Spi2A, and that Spi2A determines the level and HSP of T_{CM} by protecting these cells from intracellular cathepsin B.

The greatest reduction of Spi2A-deficient memory $CD8^+$ T cells occurred in the bone marrow, a major reservoir for T_{CM} (10). The bone marrow is also the predominant site of memory $CD8^+$ T cell homeostatic proliferation due to signals provided by the organ microenvironment (8, 9). For full turnover, memory $CD8^+$ T cells must receive the IL-15 signal trans-presented by these niches (56, 61). Consistent with this, the decline and reduced homeostatic proliferation of memory $CD8^+$ T cells seen in IL-15 KO mice resembles that observed in Spi2A KO mice (56, 58). In addition, we did not observe a significant increase in the basal level of PCD in either memory-phenotype or antigen-specific memory $CD8^+$ T cells from Spi2A KO mice, as evidenced by staining with the apoptosis dyes Annexin V or YoPro1 (Supplemental Figures 3B and 3C). However, given the well-documented anti-apoptotic function of Spi2A (29, 31), a subtle increase in PCD (below our level of detection in *ex vivo* memory T cells) is still the most likely for the decreased HSP of Spi2A KO memory cells. Our findings support a model in which IL-7 and IL-15 control memory $CD8^+$ T cell survival through protection by Spi2A from cathepsin B.

A variety of apoptotic stimuli can induce lysosomes to release their contents, including cathepsin B, into the cytosol, where they trigger PCD (27). Our results suggest that, not only is the lysosomal pathway of cell death involved in pathological processes (27), but it also plays a physiological role in the resting homeostasis of central memory $CD8^+$ T cells. The ability of Spi2A to inhibit cytosolic cathepsin B activity for full memory $CD8^+$ T cell maintenance would be particularly important in multiple natural infections with viruses or certain vaccination regimes. Thus, the identification of Spi2A as a survival factor would predict that pharmacological inhibition of cathepsins (29, 62) could potentially increase the population of persisting long-lived memory $CD8^+$ T cells, leading to less attrition over time and prevention of chronic viral infections.

Supplementary Material

Refer to Web version on PubMed Central for supplementary material.

Acknowledgments

We thank M. Birrell for hematology analysis, and N. Liu, M. Zhang, and L. Levine for their help in generating the Spi2A KO mice.

Abbreviations used in this paper

BM	bone marrow
HSP	homeostatic proliferation
ILN	inguinal lymph node
IHL	intrahepatic lymphocyte
KLRG1	killer cell lectin-like receptor G1
KO	knockout
LCMV	lymphocytic choriomeningitis virus
PCD	programmed cell death
p.i.	post infection
Spi, serpin	serine protease inhibitor
WT	wild type

References

1. Sprent J, Surh CD. T cell memory. Annu Rev Immunol. 2002; 20:551–579. [PubMed: 11861612]
2. Welsh RM, Selin LK. No one is naive: the significance of heterologous T-cell immunity. Nat Rev Immunol. 2002; 2:417–426. [PubMed: 12093008]
3. Intlekofer AM, Takemoto N, Wherry EJ, Longworth SA, Northrup JT, Palanivel VR, Mullen AC, Gasink CR, Kaech SM, Miller JD, Gapin L, Ryan K, Russ AP, Lindsten T, Orange JS, Goldrath AW, Ahmed R, Reiner SL. Effector and memory CD8+ T cell fate coupled by T-bet and eomesodermin. Nat Immunol. 2005; 6:1236–1244. [PubMed: 16273099]
4. Wherry EJ, Teichgraber V, Becker TC, Masopust D, Kaech SM, Antia R, von Andrian UH, Ahmed R. Lineage relationship and protective immunity of memory CD8 T cell subsets. Nat Immunol. 2003; 4:225–234. [PubMed: 12563257]
5. Joshi NS, Cui W, Chandele A, Lee HK, Urso DR, Hagman J, Gapin L, Kaech SM. Inflammation directs memory precursor and short-lived effector CD8(+) T cell fates via the graded expression of T-bet transcription factor. Immunity. 2007; 27:281–295. [PubMed: 17723218]

6. Sallusto F, Lenig D, Forster R, Lipp M, Lanzavecchia A. Two subsets of memory T lymphocytes with distinct homing potentials and effector functions. Nature. 1999; 401:708–712. [PubMed: 10537110]
7. Masopust D, Vezys V, Marzo AL, Lefrancois L. Preferential localization of effector memory cells in nonlymphoid tissue. Science. 2001; 291:2413–2417. [PubMed: 11264538]
8. Becker TC, Coley SM, Wherry EJ, Ahmed R. Bone marrow is a preferred site for homeostatic proliferation of memory CD8 T cells. J Immunol. 2005; 174:1269–1273. [PubMed: 15661882]
9. Cassese G, Parretta E, Pisapia L, Santoni A, Guardiola J, Di Rosa F. Bone marrow CD8 cells down-modulate membrane IL-7Ralpha expression and exhibit increased STAT-5 and p38 MAPK phosphorylation in the organ environment. Blood. 2007; 110:1960–1969. [PubMed: 17510323]
10. Mazo IB, Honczarenko M, Leung H, Cavanagh LL, Bonasio R, Weninger W, Engelke K, Xia L, McEver RP, Koni PA, Silberstein LE, von Andrian UH. Bone marrow is a major reservoir and site of recruitment for central memory CD8+ T cells. Immunity. 2005; 22:259–270. [PubMed: 15723813]
11. Tokoyoda K, Zehentmeier S, Hegazy AN, Albrecht I, Grun JR, Lohning M, Radbruch A. Professional memory CD4+ T lymphocytes preferentially reside and rest in the bone marrow. Immunity. 2009; 30:721–730. [PubMed: 19427242]
12. Hildeman D, Jorgensen T, Kappler J, Marrack P. Apoptosis and the homeostatic control of immune responses. Curr Opin Immunol. 2007; 19:516–521. [PubMed: 17644328]
13. Opferman JT, Letai A, Beard C, Sorcinelli MD, Ong CC, Korsmeyer SJ. Development and maintenance of B and T lymphocytes requires antiapoptotic MCL-1. Nature. 2003; 426:671–676. [PubMed: 14668867]
14. Sabbagh L, Pulle G, Liu Y, Tsitsikov EN, Watts TH. ERK-dependent Bim modulation downstream of the 4-1BB-TRAF1 signaling axis is a critical mediator of CD8 T cell survival in vivo. J Immunol. 2008; 180:8093–8101. [PubMed: 18523273]
15. Neuenhahn M, Busch DH. The quest for CD8+ memory stem cells. Immunity. 2009; 31:702–704. [PubMed: 19932070]
16. Dennemarker J, Lohmuller T, Muller S, Aguilar SV, Tobin DJ, Peters C, Reinheckel T. Impaired turnover of autophagolysosomes in cathepsin L deficiency. Biol Chem. 2010
17. Zavasnik-Bergant T, Turk B. Cysteine proteases: destruction ability versus immunomodulation capacity in immune cells. Biol Chem. 2007; 388:1141–1149. [PubMed: 17976006]
18. Foghsgaard L, Wissing D, Mauch D, Lademann U, Bastholm L, Boes M, Elling F, Leist M, Jaattela M. Cathepsin B acts as a dominant execution protease in tumor cell apoptosis induced by tumor necrosis factor. J. Cell Biol. 2001; 153:999–1009. [PubMed: 11381085]
19. Guicciardi ME, Deussing J, Miyoshi H, Bronk SF, Svingen PA, Peters C, Kaufmann SH, Gores GJ. Cathepsin B contributes to TNF-alpha-mediated hepatocyte apoptosis by promoting mitochondrial release of cytochrome c. J Clin Invest. 2000; 106:1127–1137. [PubMed: 11067865]
20. Guicciardi ME, Miyoshi H, Bronk SF, Gores GJ. Cathepsin B knockout mice are resistant to tumor necrosis factor-alpha-mediated hepatocyte apoptosis and liver injury: implications for therapeutic applications. Am J Pathol. 2001; 159:2045–2054. [PubMed: 11733355]
21. Roberg K, Johansson U, Ollinger K. Lysosomal release of cathepsin D precedes relocation of cytochrome c and loss of mitochondrial transmembrane potential during apoptosis induced by oxidative stress. Free Radic Biol Med. 1999; 27:1228–1237. [PubMed: 10641715]
22. Roberg K, Ollinger K. Oxidative stress causes relocation of the lysosomal enzyme cathepsin D with ensuing apoptosis in neonatal rat cardiomyocytes. Am J Pathol. 1998; 152:1151–1156. [PubMed: 9588882]
23. Zhao M, Antunes F, Eaton JW, Brunk UT. Lysosomal enzymes promote mitochondrial oxidant production, cytochrome c release and apoptosis. Eur J Biochem. 2003; 270:3778–3786. [PubMed: 12950261]
24. Blomgran R, Zheng L, Stendahl O. Cathepsin-cleaved Bid promotes apoptosis in human neutrophils via oxidative stress-induced lysosomal membrane permeabilization. J Leukoc Biol. 2007; 81:1213–1223. [PubMed: 17264306]

25. Cirman T, Oresic K, Mazovec GD, Turk V, Reed JC, Myers RM, Salvesen GS, Turk B. Selective disruption of lysosomes in HeLa cells triggers apoptosis mediated by cleavage of Bid by multiple papain-like lysosomal cathepsins. J Biol Chem. 2004; 279:3578–3587. [PubMed: 14581476]
26. Bidere N, Lorenzo HK, Carmona S, Laforge M, Harper F, Dumont C, Senik A. Cathepsin D triggers Bax activation, resulting in selective apoptosis-inducing factor (AIF) relocation in T lymphocytes entering the early commitment phase to apoptosis. J Biol Chem. 2003; 278:31401–31411. [PubMed: 12782632]
27. Kroemer G, Jaattela M. Lysosomes and autophagy in cell death control. Nat Rev Cancer. 2005; 5:886–897. [PubMed: 16239905]
28. Droga-Mazovec G, Bojic L, Petelin A, Ivanova S, Romih R, Repnik U, Salvesen GS, Stoka V, Turk V, Turk B. Cysteine cathepsins trigger caspase-dependent cell death through cleavage of bid and antiapoptotic Bcl-2 homologues. J Biol Chem. 2008; 283:19140–19150. [PubMed: 18469004]
29. Liu N, Phillips T, Zhang M, Wang Y, Opferman JT, Shah R, Ashton-Rickardt PG. Serine protease inhibitor 2A is a protective factor for memory T cell development. Nat Immunol. 2004; 5:919–926. [PubMed: 15311278]
30. Forsyth S, Horvath A, Coughlin P. A review and comparison of the murine alpha1-antitrypsin and alpha1-antichymotrypsin multigene clusters with the human clade A serpins. Genomics. 2003; 81:336–345. [PubMed: 12659817]
31. Liu N, Raja SM, Zazzeroni F, Metkar SS, Shah R, Zhang M, Wang Y, Bromme D, Russin WA, Lee JC, Peter ME, Froelich CJ, Franzoso G, Ashton-Rickardt PG. NF-kappaB protects from the lysosomal pathway of cell death. Embo J. 2003; 22:5313–5322. [PubMed: 14517268]
32. Dev A, Byrne SM, Ashton-Rickardt PG, Wojchowski DM. EPO Cytoprotects erythroblasts from oxidative stress via serpin-mediated inhibition of lysosomal cathepsins. Nat Med. 2011 (under review, manuscript attached).
33. Pircher H, Burki K, Lang R, Hengartner H, Zinkernagel RM. Tolerance induction in double specific T-cell receptor transgenic mice varies with antigen. Nature. 1989; 342:559–561. [PubMed: 2573841]
34. Deussing J, Roth W, Saftig P, Peters C, Ploegh HL, Villadangos JA. Cathepsins B and D are dispensable for major histocompatibility complex class II-mediated antigen presentation. Proc Natl Acad Sci U S A. 1998; 95:4516–4521. [PubMed: 9539769]
35. Winkler IG, Hendy J, Coughlin P, Horvath A, Levesque JP. Serine protease inhibitors serpina1 and serpina3 are down-regulated in bone marrow during hematopoietic progenitor mobilization. J Exp Med. 2005; 201:1077–1088. [PubMed: 15795238]
36. Zhang M, Byrne S, Liu N, Wang Y, Oxenius A, Ashton-Rickardt PG. Differential survival of cytotoxic T cells and memory cell precursors. J Immunol. 2007; 178:3483–3491. [PubMed: 17339443]
37. Gill SC, von Hippel PH. Calculation of protein extinction coefficients from amino acid sequence data. Anal Biochem. 1989; 182:319–326. [PubMed: 2610349]
38. Barrett AJ, Kembhavi AA, Brown MA, Kirschke H, Knight CG, Tamai M, Hanada K. L-trans-Epoxysuccinyl-leucylamido(4-guanidino)butane (E-64) and its analogues as inhibitors of cysteine proteinases including cathepsins B, H and L. Biochem J. 1982; 201:189–198. [PubMed: 7044372]
39. Patston PA, Church FC, Olson ST. Serpin-ligand interactions. Methods. 2004; 32:93–109. [PubMed: 14698622]
40. Tough DF, Sprent J. Turnover of Naive- and Memory-phenotype T Cells. J Exp Med. 1994; 179:1127–1135. [PubMed: 8145034]
41. Miller RA. Age-related changes in T cell surface markers: a longitudinal analysis in genetically heterogeneous mice. Mech Ageing Dev. 1997; 96:181–196. [PubMed: 9223120]
42. Parretta E, Cassese G, Barba P, Santoni A, Guardiola J, Di Rosa F. CD8 cell division maintaining cytotoxic memory occurs predominantly in the bone marrow. J Immunol. 2005; 174:7654–7664. [PubMed: 15944266]
43. Surh CD, Sprent J. Homeostasis of naive and memory T cells. Immunity. 2008; 29:848–862. [PubMed: 19100699]

44. Hikono H, Kohlmeier JE, Takamura S, Wittmer ST, Roberts AD, Woodland DL. Activation phenotype, rather than central- or effector-memory phenotype, predicts the recall efficacy of memory CD8+ T cells. J Exp Med. 2007; 204:1625–1636. [PubMed: 17606632]
45. Waterstrat A, Liang Y, Swiderski CF, Shelton BJ, Van Zant G. Congenic interval of CD45 / Ly-5 congenic mice contains multiple genes that may influence hematopoietic stem cell engraftment. Blood. 2009
46. Chwieralski CE, Welte T, Buhling F. Cathepsin-regulated apoptosis. Apoptosis. 2006; 11:143–149. [PubMed: 16502253]
47. Werneburg NW, Guicciardi ME, Bronk SF, Gores GJ. Tumor necrosis factor-alpha-associated lysosomal permeabilization is cathepsin B dependent. Am J Physiol Gastrointest Liver Physiol. 2002; 283:G947–956. [PubMed: 12223355]
48. Boya P, Andreau K, Poncet D, Zamzami N, Perfettini JL, Metivier D, Ojcius DM, Jaattela M, Kroemer G. Lysosomal membrane permeabilization induces cell death in a mitochondrion-dependent fashion. J Exp Med. 2003; 197:1323–1334. [PubMed: 12756268]
49. Jolly C, Sattentau QJ. Regulated secretion from CD4+ T cells. Trends Immunol. 2007; 28:474–481. [PubMed: 17962070]
50. Gettins PG. Serpin structure, mechanism, and function. Chem Rev. 2002; 102:4751–4804. [PubMed: 12475206]
51. Irving JA, Pike RN, Dai W, Bromme D, Worrall DM, Silverman GA, Coetzer TH, Dennison C, Bottomley SP, Whisstock JC. Evidence that serpin architecture intrinsically supports papain-like cysteine protease inhibition: engineering alpha(1)-antitrypsin to inhibit cathepsin proteases. Biochemistry. 2002; 41:4998–5004. [PubMed: 11939796]
52. Silverman GA, Bird PI, Carrell RW, Church FC, Coughlin PB, Gettins PGW, Irving JA, Lomas DA, Luke CJ, Moyer RW, Pemberton PA, Remold-O'Donnell E, Salvesen GS, Travis J, Whisstock JC. The serpins are an expanding superfamily of structurally similar but functionally diverse proteins. J.Biol.Chem. 2001; 276:33293–33296. [PubMed: 11435447]
53. Boya P, Mellen MA, de la Rosa EJ. How autophagy is related to programmed cell death during the development of the nervous system. Biochem Soc Trans. 2008; 36:813–817. [PubMed: 18793142]
54. Zhang M, Park SM, Wang Y, Shah R, Liu N, Murmann AE, Wang CR, Peter ME, Ashton-Rickardt PG. Serine protease inhibitor 6 protects cytotoxic T cells from self-inflicted injury by ensuring the integrity of cytotoxic granules. Immunity. 2006; 24:451–461. [PubMed: 16618603]
55. Vezys V, Yates A, Casey KA, Lanier G, Ahmed R, Antia R, Masopust D. Memory CD8 T-cell compartment grows in size with immunological experience. Nature. 2009; 457:196–199. [PubMed: 19005468]
56. Becker TC, Wherry EJ, Boone D, Murali-Krishna K, Antia R, Ma A, Ahmed R. Interleukin 15 is required for proliferative renewal of virus-specific memory CD8 T cells. J Exp Med. 2002; 195:1541–1548. [PubMed: 12070282]
57. Schluns KS, Kieper WC, Jameson SC, Lefrancois L. Interleukin-7 mediates the homeostasis of naive and memory CD8 T cells in vivo. Nat Immunol. 2000; 1:426–432. [PubMed: 11062503]
58. Schluns KS, Williams K, Ma A, Zheng XX, Lefrancois L. Cutting edge: requirement for IL-15 in the generation of primary and memory antigen-specific CD8 T cells. J Immunol. 2002; 168:4827–4831. [PubMed: 11994430]
59. Petschner F, Zimmerman C, Strasser A, Grillot D, Nunez G, Pircher H. Constitutive expression of Bcl-xL or Bcl-2 prevents peptide antigen-induced T cell deletion but does not influence T cell homeostasis after a viral infection. Eur J Immunol. 1998; 28:560–569. [PubMed: 9521066]
60. Razvi ES, Jiang Z, Woda BA, Welsh RM. Lymphocyte apoptosis during the silencing of the immune response to acute viral infections in normal, lpr, and Bcl-2-transgenic mice. Am J Pathol. 1995; 147:79–91. [PubMed: 7604887]
61. Ma A, Koka R, Burkett P. Diverse functions of IL-2, IL-15, and IL-7 in lymphoid homeostasis. Annu Rev Immunol. 2006; 24:657–679. [PubMed: 16551262]
62. Michallet MC, Saltel F, Flacher M, Revillard JP, Genestier L. Cathepsin-dependent apoptosis triggered by supraoptimal activation of T lymphocytes: a possible mechanism of high dose tolerance. J Immunol. 2004; 172:5405–5414. [PubMed: 15100281]

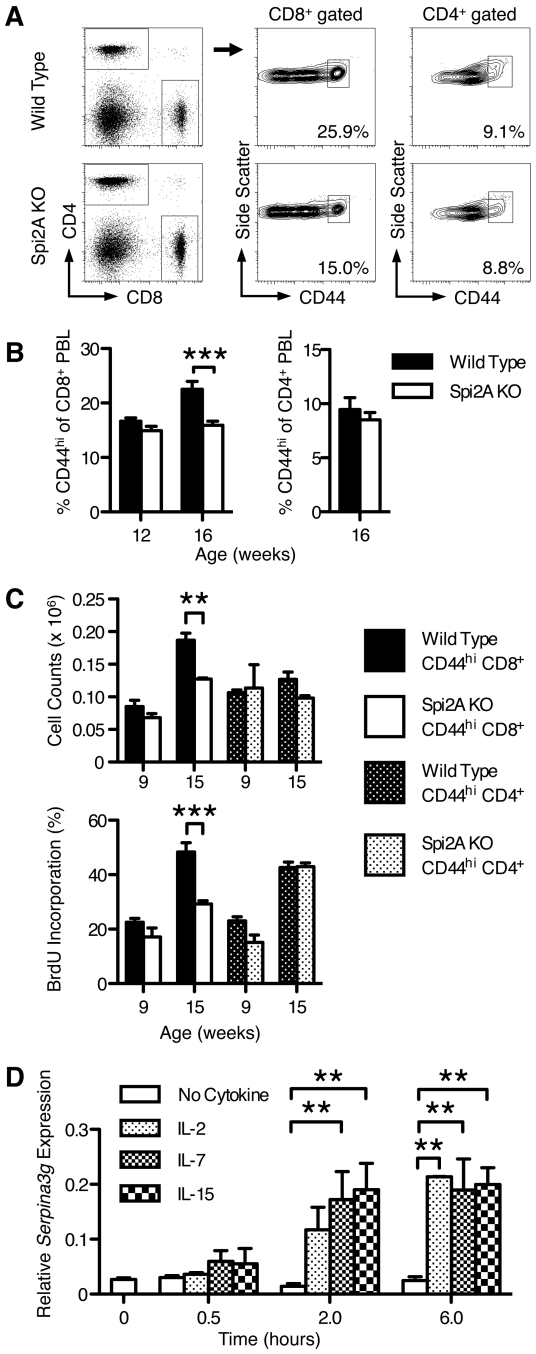

Figure 1. Spi2A-deficient mice develop fewer memory-phenotype CD44^{hi} CD8^{+} T cells

(**A**) Representative flow cytometry staining of CD44^{hi} CD8^{+} and CD44^{hi} CD4^{+} T cells in the blood of 16-week-old wild type or Spi2A KO mice. (**B**) Proportion of CD44^{hi} cells in the CD8^{+} or CD4^{+} T cell populations. (**C**) Upper row: Number of CD44^{hi} CD8^{+} or CD44^{hi} CD4^{+} T cells present in one femur of 9- and 15-week-old mice. Lower row: BrdU incorporation of CD44^{hi} CD8^{+} and CD44^{hi} CD4^{+} T cells after one week of BrdU administration in 9- and 15-week-old mice. (**A-C**) Data show mean ± SEM of at least n = 5 mice. (**D**) CD44^{hi} CD8^{+} cells were purified by magnetic microbeads and FACS sorting from three samples each consisting of three spleens from pooled wild type mice. Cells were

cultured in complete DMEM-10 without cytokine for 4 hours, and then cultured in 100 ng / ml cytokine for the indicated times. *Serpina3g* expression was assayed by real time PCR and shown relative to *β2microglobulin* expression levels. (**A-D**) Significance values were calculated by two-way ANOVA with Bonferroni post-test (*, $P < 0.05$, **, $P < 0.01$, ***, $P < 0.001$). Results are representative of at least two independent experiments.

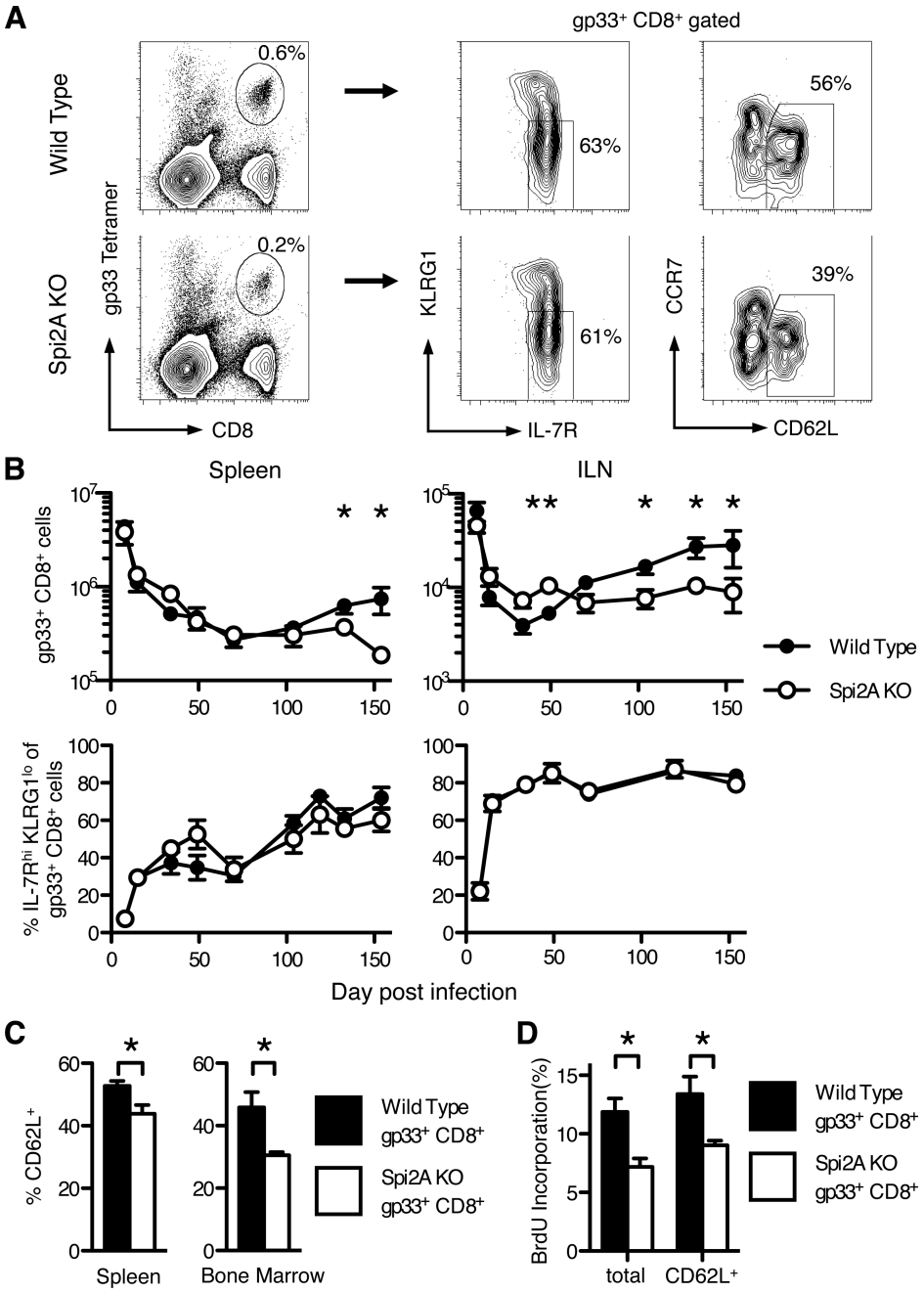

Figure 2. Spi2A KO mice have fewer memory CD8$^+$ T cells after LCMV infection

Wild type and Spi2A KO mice were infected with LCMV Armstrong and dissected 130 days post infection. (**A**) Representative flow cytometry staining of wild type and Spi2A KO splenocytes. Leukocytes were gated for CD8 expression and a tetramer specific for the gp33 immunodominant LCMV epitope, and then further analyzed for memory markers: IL-7R and KLRG1, and CD62L and CCR7. (**B**) Number of gp33$^+$ CD8$^+$ cells (upper row) and proportion of IL-7R^{hi} KLRG1^{lo} cells within the gp33$^+$ CD8$^+$ population (lower row) over time in the spleen and both inguinal lymph nodes (ILN). (**C**) Proportion of CD62L$^+$ (T_{CM}) cells within the gp33$^+$ CD8$^+$ population in the spleen and bone marrow. (**D**) BrdU incorporation of total gp33$^+$ CD8$^+$ cells and CD62L$^+$ gp33$^+$ CD8$^+$ cells after one week of

BrdU administration. Data show mean ± SEM of at least n = 4 mice. Significance values were calculated by Student's two-tailed t-test (*, $P < 0.05$, **, $P < 0.01$). Results are representative of at least 2 independent experiments.

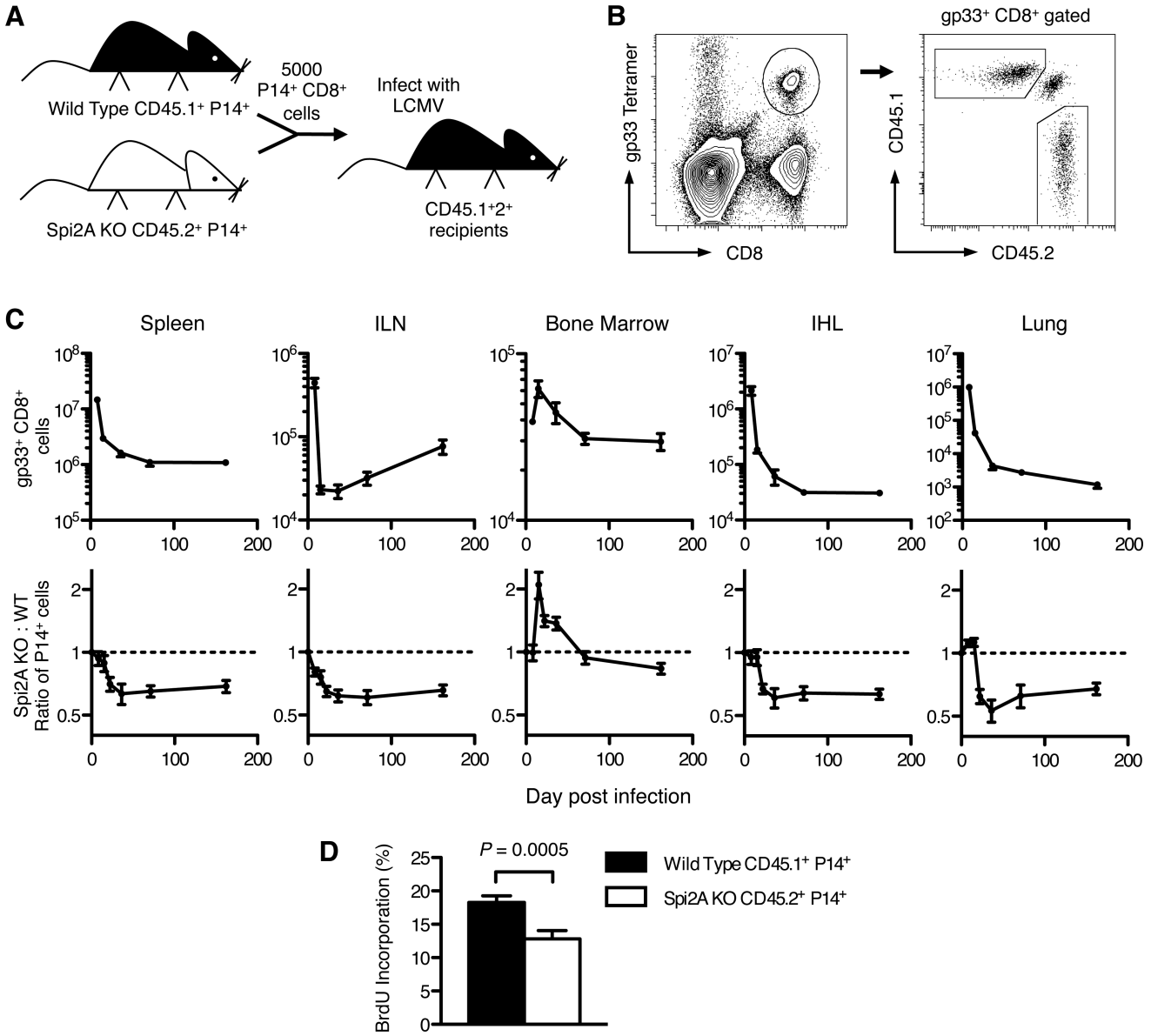

Figure 3. Cell intrinsic impaired maintenance of Spi2A-deficient CD8$^+$ memory T cells after viral infection

CD8$^+$ splenocytes from gp33 epitope-specific P14 TCR transgenic wild type (WT, CD45.1$^+$) mice and Spi2A KO (CD45.2$^+$) mice were isolated and mixed in an even ratio. 5000 P14$^+$ CD8$^+$ cells were adoptively transferred into CD45.1$^+$2$^+$ hybrid congenic recipients, which were subsequently infected with LCMV. (**A**) Competitive adoptive transfer experiment. (**B**) Flow cytometry analysis of gp33$^+$ CD8$^+$ splenocytes showing CD45.1$^+$ (WT) donor, CD45.2$^+$ (KO) donor, and CD45.1$^+$2$^+$ endogenous populations. (**C**) Upper row: Total number of gp33$^+$ CD8$^+$ cells in various organs after LCMV infection. (ILN: both inguinal lymph nodes; bone marrow from one femur; IHL: intrahepatic lymphocytes) Lower row: Ratio of Spi2A KO: Wild Type among donor P14$^+$ CD8$^+$ cells. Initial ratio of 1 is indicated by dotted line. (**D**) BrdU incorporation of P14$^+$ CD8$^+$ cells in bone marrow after one week of BrdU administration in mice 70-75 days post infection. Significance values were calculated by paired Student's two-tailed t test. Data show mean ± SEM of at least n = 6 mice. Results are representative of at least 2 independent experiments.

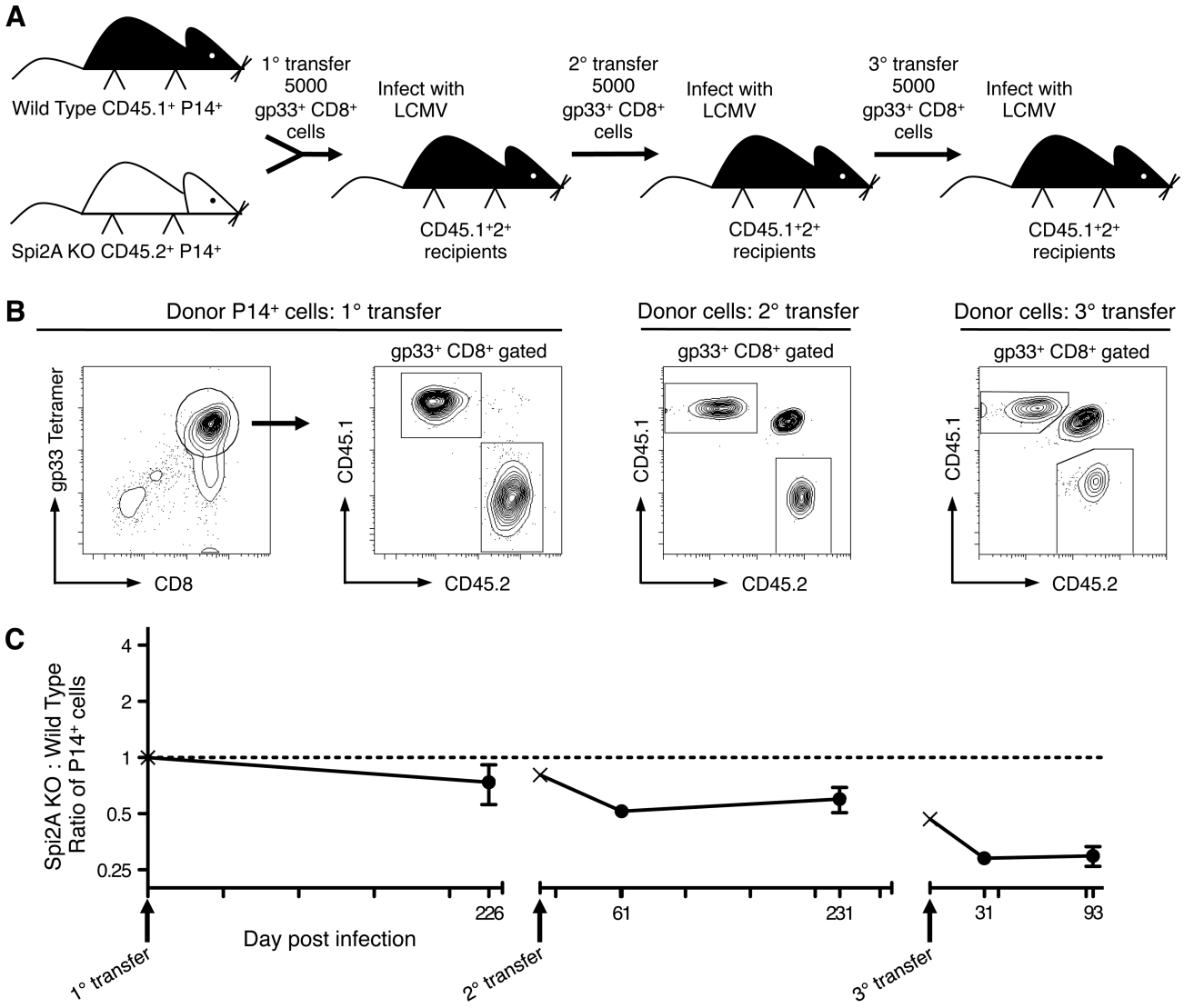

Figure 4. Spi2A-deficient CD8$^+$ memory T cells decline with successive infections

CD8$^+$ splenocytes from gp33 epitope-specific P14 transgenic wild type CD45.1$^+$ mice and Spi2A KO CD45.2$^+$ mice were isolated and mixed in an even ratio. 5000 P14$^+$ CD8$^+$ cells were adoptively transferred into CD45.1$^+$2$^+$ hybrid congenic recipients, which were subsequently infected with LCMV (1° transfer). Greater than 200 days post infection, 5000 P14$^+$ CD8$^+$ splenocytes were isolated from these mice and adoptively transferred into new CD45.1$^+$2$^+$ recipients, which were subsequently infected with LCMV (2° transfer). This procedure was then repeated a third time (3° transfer). (**A**) Successive competitive adoptive transfer experiment. (**B**) Flow cytometry profiles of purified CD8$^+$ splenocytes injected for each transfer. (**C**) Ratio of Spi2A KO : Wild Type among donor P14$^+$ CD8$^+$ PBL. Initial ratio of 1 is indicated by dotted line. Arrows indicate time of each transfer. The P14 ratio of each injected transplant is marked by ×. Data show mean ± SEM of 8-30 mice.

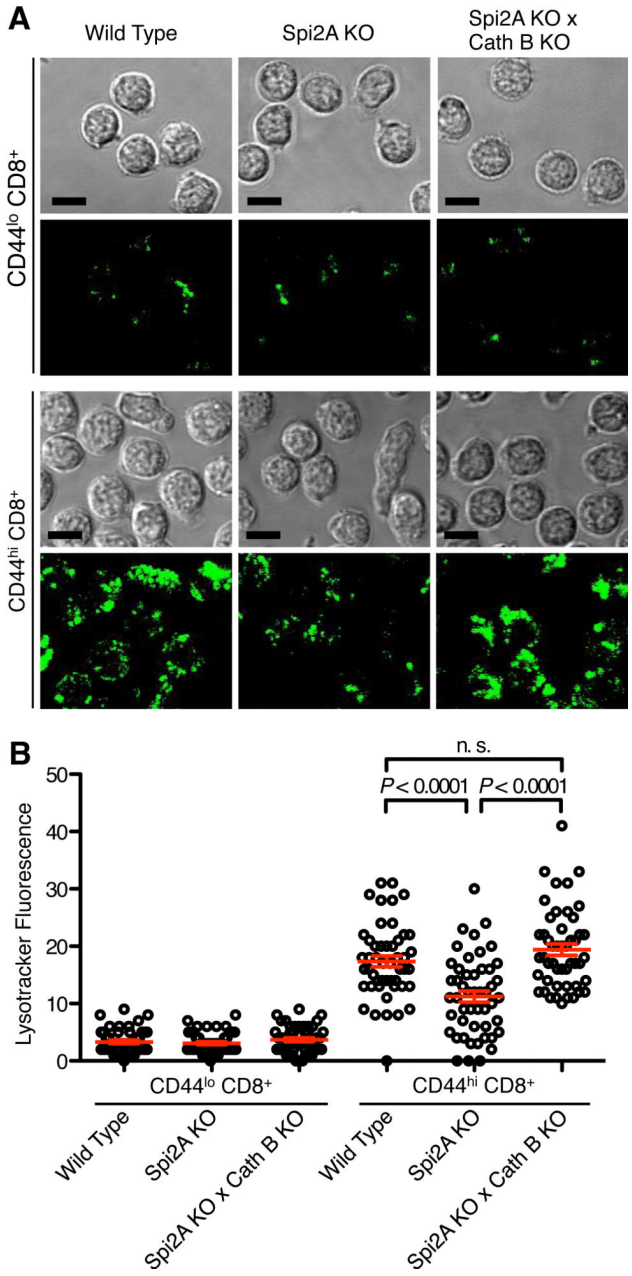

Figure 5. Spi2A KO memory-phenotype CD8$^+$ T cells have fewer intact lysosomes

(**A**) Acidic lysosomes were visualized by staining *ex vivo* FACS-purified CD44^{lo} CD8$^+$ and CD44^{hi} CD8$^+$ splenocytes from Wild Type, Spi2A KO, and Spi2A KO × Cath B KO mice with Lysotracker Green DND-26. Panels show the transmission image of representative cells (n > 200) and a merged image of several optical slices taken every micron throughout the cells to depict the total Lysotracker fluorescence. The scale bars represent 10 μm. (**B**) The mean fluorescence (total fluorescence / volume of the cell) was determined in the different cell types (n = 49 for each cell type). Mean values are shown by the red bar (***, $P < 0.0001$, n.s. not significant $P > 0.05$). This diagram is representative of 3 independent experiments.

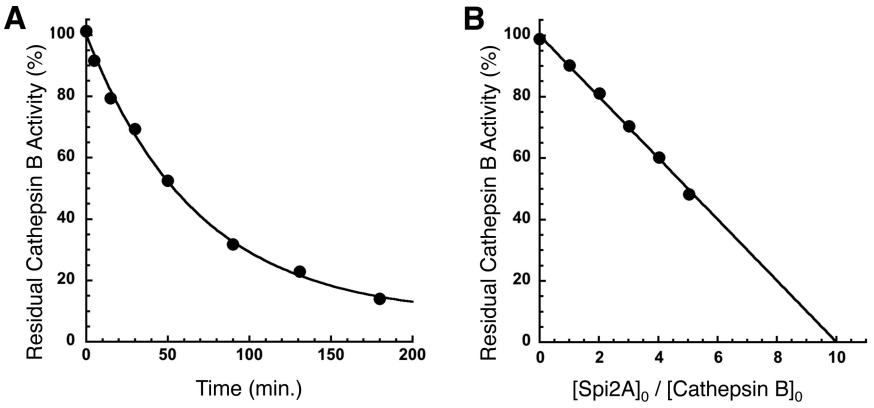

C

	k_a ($M^{-1}s^{-1}$)	SI	Corrected k_a ($M^{-1}s^{-1}$)
Cathepsin B	6×10^2	10:1	6×10^3
Cathepsin H	5×10^2	1:1	5×10^2
Cathepsin K	2×10^5	8:1	2×10^6
Cathepsin L	6×10^4	6:1	4×10^5
Cathepsin S	5×10^4	20:1	1×10^6
Cathepsin V	3×10^5	20:1	6×10^6
Papain	4×10^0	ND	ND

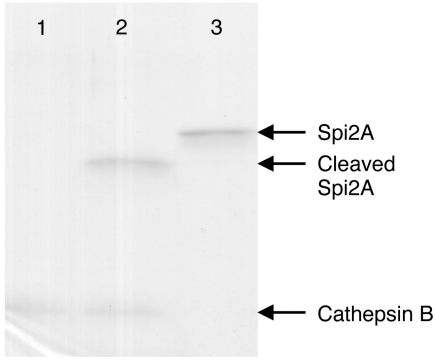

Figure 6. Kinetics and stoichiometry of cathepsin inhibition by Spi2A

(**A**) Progress curve for the inhibition of cathepsin B (5 nM) by Spi2A (440 nM). The solid line is a fit by a single exponential decay function. (**B**) Cathepsin B (100 nM) was incubated with the indicated molar ratios of Spi2A for a time sufficient to reach the reaction endpoint and then assayed for residual enzyme activity as in the kinetics experiment. The x-axis intercept of the solid linear regression fit of the data represents the stoichiometry of inhibition. (**C**) Second order rate constants and stoichiometries of inhibition (SI) for the reactions of Spi2A with different cathepsins. The corrected second order rate constants for reaction through the inhibitory pathway were obtained by multiplying the apparent second order rate constant by the stoichiometry of inhibition (50). (**D**) SDS-PAGE analysis (10% gel) of the reaction of Spi2A with cathepsin B. Shown are 0.5 μM cathepsin B alone (lane 1), 2 μM Spi2A with 0.5 μM cathepsin B reacted for 90 min. (lane 2), and 2 μM Spi2A alone (lane 3). Intact cathepsin B and cleaved Spi2A are the only visible products of the reaction because of the instability of serpin-cysteine protease complexes to SDS denaturation.

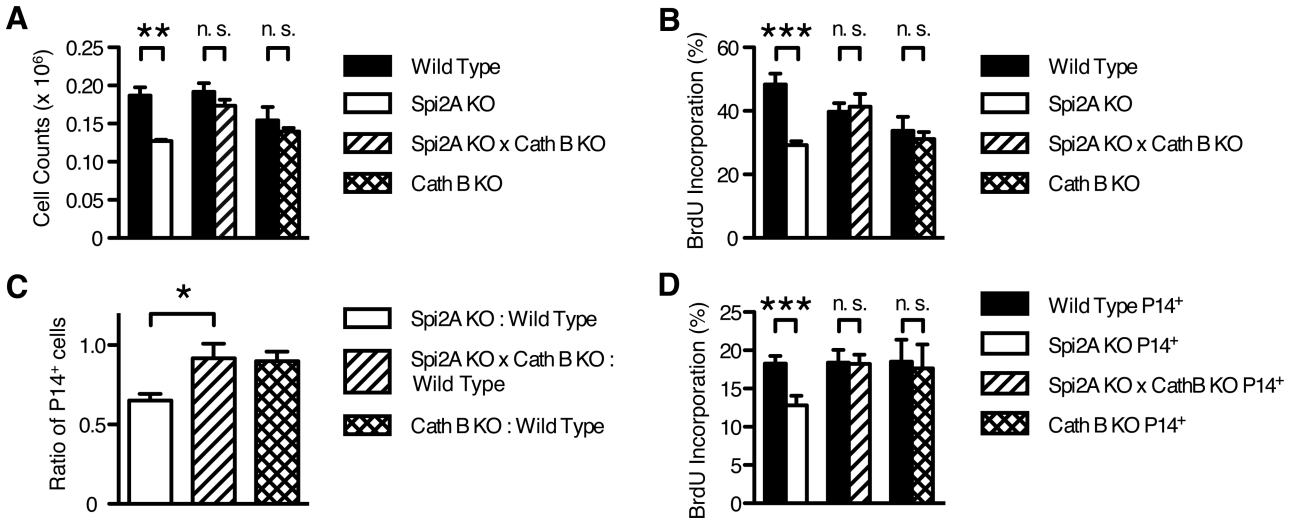

Figure 7. Concomitant cathepsin B deficiency restores the reduced number and homeostatic proliferation of Spi2A-deficient memory-phenotype CD44^{hi} CD8^{+} and memory CD8^{+} T cells

(**A-B**) 15-week-old mice were dissected and stained as in Figure 1. (**A**) Number of CD44^{hi} CD8^{+} T cells present in one femur. (**B**) BrdU incorporation of CD44^{hi} CD8^{+} T cells after one week of BrdU administration. Significance values were calculated by two-way ANOVA with Bonferroni post-test (**, $P < 0.01$; ***, $P < 0.001$). (**C-D**) CD8^{+} splenocytes from gp33 epitope-specific P14 TCR transgenic wild type (CD45.1^{+}) mice and either Spi2A KO, Spi2A KO × Cath B KO, or Cath B KO (CD45.2^{+}) mice were isolated and mixed in even ratios. 5000 P14^{+} CD8^{+} cells were adoptively transferred into CD45.1^{+}2^{+} hybrid congenic recipients, which were subsequently infected with LCMV, as described in Figure 3. (**C**) Ratio of Spi2A KO, Spi2A × Cath B KO, or Cath B KO : Wild Type among donor P14^{+} CD8^{+} cells in the spleen 70-76 days post infection. Significance values were calculated by one-way ANOVA with Bonferroni post-test (*, $P < 0.05$). (**D**) BrdU incorporation of P14^{+} CD8^{+} cells in spleen and bone marrow after one week of BrdU administration in mice 70-75 days post infection. Significance values were calculated by paired Student's two-tailed t test (***, $P < 0.001$). (**A-D**) Data show mean ± SEM of at least n = 5 mice and are representative of at least 2 independent experiments.

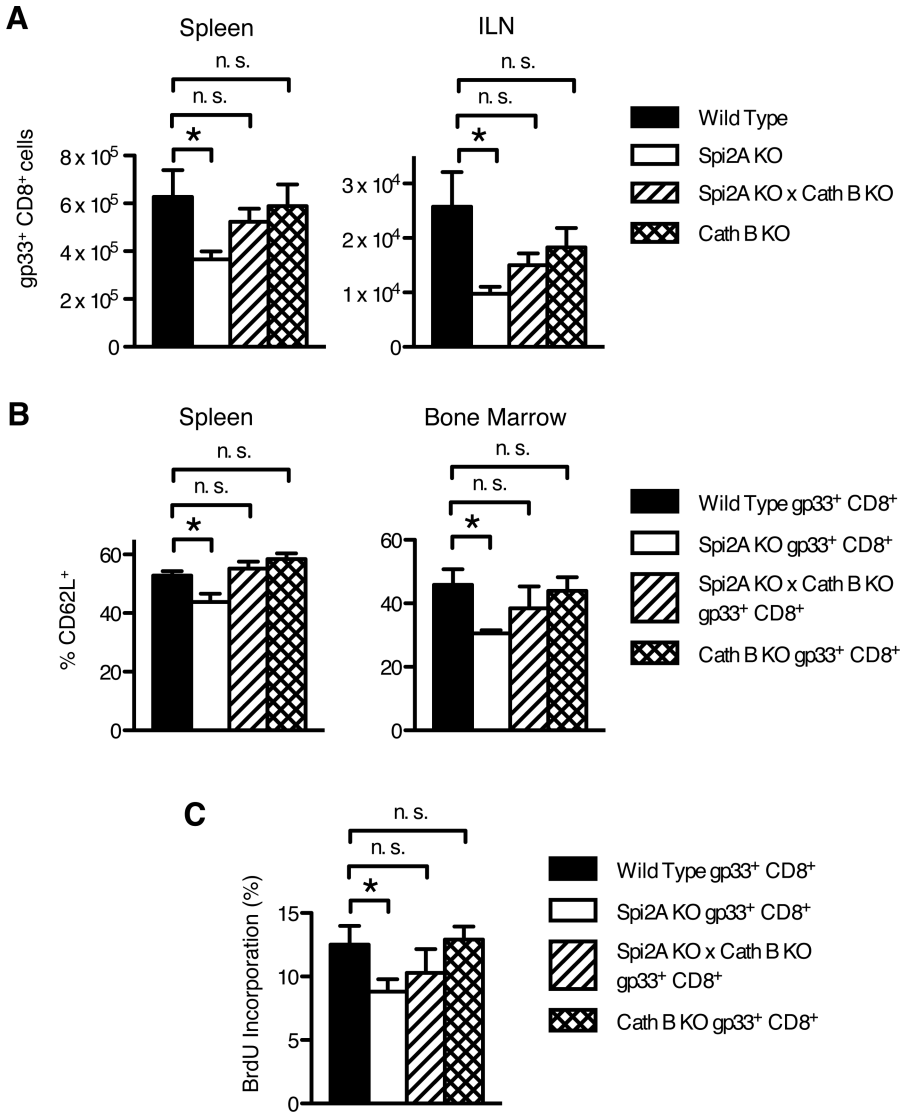

Figure 8. Concomitant cathepsin B deficiency restores the number and homeostatic proliferation of Spi2A KO memory CD8$^+$ T cells after LCMV infection

Mice were infected with LCMV Armstrong and dissected 130 days post infection. (**A**) Number of memory gp33$^+$ CD8$^+$ cells in the spleen and both inguinal lymph nodes (ILN). (**B**) Proportion of CD62L$^+$ T_{CM} cells within the memory gp33$^+$ CD8$^+$ population in the spleen and bone marrow. (**C**) BrdU incorporation of total gp33$^+$ CD8$^+$ cells after one week of BrdU administration. Data show mean ± SEM of at least n = 4 mice. Significance values were calculated by Student's two-tailed t-test (*, $P < 0.05$, **, $P < 0.01$, n.s. not significant $P > 0.05$).